Role of magnetic field on forced convection of nanofluid in a branching channel

Fatih Selimefendigil
Department of Mechanical Engineering, Celal Bayar University, Manisa, Turkey
Hakan F. Öztop
Department of Mechanical Engineering, Firat University, Elazig, Turkey, and
Ali J. Chamkha
Department of Mechanical Engineering, Prince Mohammad Bin Fahd University, Al-Khobar, Saudi Arabia

Received 11 October 2018
Revised 15 November 2018
Accepted 26 November 2018

Abstract

Purpose – Numerical study of nanofluid forced convection within a branching channel was performed under the influence of a uniform magnetic field. The purpose of this study is to enhance the heat transfer performance of the separated flow at the branching channel with the use of magnetic field and nanofluid. The use of magnetic field and enhancement in both the thermal conductivity and electrical conductivity with the inclusion of the nanoparticles provides favorable thermophysical properties of the nanofluid when it used as a heat transfer fluid in a branching channel. The results of this study may be used to control the thermal performance in a branching channel and further optimization studies in the presence of magnetic field.

Design/methodology/approach – Galerkin weighted residual finite element method was used for the simulations. The numerical simulation results are performed by changing the inclination angle of the lower branching channel (between 0° and 90°), thermophysical properties of the fluid via inclusion of nanoparticles (between 0 and 0.04), Reynolds number (between 100 and 400) and magnetic field strength (Hartmann number changes between 0 and 15).

Findings – It was observed that the recirculation zones and reattachment length of the upper and lower branching channels are affected by the variation of those parameters. Reattachment lengths increase with the augmentation of the Reynolds number and deterioration of the Hartmann number. Average Nusselt number becomes higher for higher values of Hartmann number and solid particle volume fraction. Inclusion of the nanoparticle to the base fluid is very effective for the configuration with higher values of Hartmann number. An optimum value of the inclination angle of the lower branching channel is observed, beyond which heat transfer rate is significantly reduced due to the establishment of a large vortex in the upper branching channel and restriction of the fluid motion.

Originality/value – In this study, forced convection of nanofluid flow in a branching channel under the effect of magnetic field was numerically studied. Magnetic field effects with nanoparticle inclusion to the base fluid on the convective heat transfer was analyzed for various inclination angles of the lower branching channel. Flow separation at the junction of the channels and thus convective heat transfer rate are influenced by the variation of these parameters. There are many studies related to application of the magnetic field with nanofluids, and a few of them are related to configurations with separated flows. To the best of the authors' knowledge, there exist no studies for the application of nanofluids and magnetic field for the convective heat transfer in a branching channel. This topic is of importance as there are many engineering applications of the branching channels.

Keywords Finite element method, Nanofluid

Paper type Research paper

International Journal of Numerical Methods for Heat & Fluid Flow

0961-5539
DOI 10.1108/HFF-10-2018-0568

Nomenclature

h = local heat transfer coefficient;
k = thermal conductivity;
H = height of the channels;
L = length of the channels;
N = unit normal vector;
Nu_x = local Nusselt number;
Nu_m = averaged Nusselt number;
p = pressure;
Pr = Prandtl number;
Re = Reynolds number;
T = temperature;
u, v = x-y velocity components;
w_k = weight function; and
x, y = Cartesian coordinates.

Greek Characters

α = thermal diffusivity;
β = expansion coefficient;
γ = magnetic inclination angle;
σ = electrical conductivity;
ϕ = solid volume fraction;
ν = kinematic viscosity;
θ = non-dimensional temperature; and
ρ = density of the fluid.

Subscripts

c = cold;
h = hot;
m = average;
nf = nanofluid;
p = solid particle; and
st = static.

1. Introduction

Fluid flow and heat transfer in a branching channel are of importance in a wide range of engineering applications such as in bio-mechanical applications, Microelectromechanical systems, gas pipelines, geothermal systems, fuel cells, chemical engineering, pharmaceutical industries and many others. The flow separation and reattachment occur in those systems. A vast amount of literature can be found for the convective heat transfer for a backward-facing step geometry where flow separation and reattachment are encountered (Abu-Mulaweh, 2003; Chiang and Sheu, 1999; Dyne *et al.*, 1993; Kaiktsis *et al.*, 1991; Lin *et al.*, 1990; Nie and Armaly, 2004; Selimefendigil and Oztop, 2013a; Selimefendigil and Oztop, 2014a; Terhaar *et al.*, 2010; Williams and Baker, 1997). (Khandelwal *et al.*, 2015) performed numerical simulations for the non-Newtonian fluid flow in a T-channel with finite volume method. Effects of various values of Reynolds number and power-law index on the recirculation regions were analyzed. In a recent study, Luo *et al.* (2018) performed a theoretical study for the heat transfer in a branch network. Effects of geometrical changes in the network such as pipe diameters, length of the pipes, ratio of the diameters on the heat

transfer characteristics were obtained. It was observed that the heat transfer rate enhances with trunk diameter and decreases with the length of the branched structure. Wang *et al.* (2010) performed 3D numerical simulation for the fluid flow and heat transfer characteristics of symmetrical and asymmetrical branching networks. It was reported that the effects of asymmetry is minor for tree-like branching network when the branching number is lower. In the study by Matos and Oliveira (2013), laminar flow of non-Newtonian inelastic fluid flow in a bifurcating channel with computational fluid dynamics simulations were performed for a range of Reynolds number, flow rate ratio and power-law index values. Fluid flow and thermal characteristics in tree-like micro-channel nets were numerically examined by (Senn and Poulikakos, 2004). Effects of secondary flow motions at bifurcations on the thermal mixing were also analyzed. In the work of Khodadadi *et al.* (1986), laminar forced convection in a two dimensional (2D), 90° bifurcating channel was numerically examined by using finite difference method. Effects of Reynolds numbers and dividing flow rates on the convective heat transfer characteristic were analyzed. The size and location of the recirculation regions established in the bifurcation were found to be affected by the variation of those parameters. In another study, Khodadadi *et al.* (1988) performed experimental study of laminar pulsating flow through a 90° bifurcation by using LDA velocity measurements. They showed the effects of Reynolds number, dividing flow rate and Stokes number on the formation of recirculating zones within the channels.

Magnetic field effects were encountered in various engineering applications such as in coolers of nuclear reactors and purification of molten metals. An external magnetic field can be used to control the convective heat transfer characteristic in different thermal engineering problems (Jang and Hsu, 2009; Rahman *et al.*, 2013; Sarris *et al.*, 2006; Selimefendigil and Chamkha, 2016; Sivasankaran *et al.*, 2016). For example, in a jet cooling application, magnetic field was used to stabilize the flow and control the heat transfer rate (Lee *et al.*, 2005). Effects of magnetic field on the convection is generally in a way to dampen the fluid motion and reduce the convective heat transfer as it is shown in many studies (Hossain and Alim, 2014; Ishak *et al.*, 2009; Oztop *et al.*, 2012). Magnetic field can also be used to control the size of the recirculation zones in separated flows and convection can be enhanced (Selimefendigil and Oztop, 2015a). Electrical conductivity of base fluids such as water can be enhanced by using nanoparticles. Recently, a new type of heat transfer fluid called nanofluid is widely used in various thermal engineering applications (Abu-Nada and Chamkha, 2010; Armaghani *et al.*, 2014; Esmaeilpour and Abdollahzadeh, 2012; Maghrebi *et al.*, 2012; Oztop and Abu-Nada, 2008; Saryazdi *et al.*, 2016; Selimefendigil *et al.*, 2017; Selimefendigil and Oztop, 2014b; Selimefendigil and Oztop, 2015b; Selimefendigil and Oztop, 2017). Nano-sized particles with an average particle size less than 100 nm are added to heat transfer fluids such as water or ethylene glycol to achieve favorable thermal properties. Thermal conductivity of the base fluid enhances even with very few amount of nanoparticle addition. Shape, size and type of the particles are effective on the thermal conductivity enhancement of the base fluid. There are various studies with the application of nanofluid for separated flows. In a previous study (Al-aswadi *et al.*, 2010), forced convective flow of nanofluids for backward-facing step geometry was analyzed for different nanofluid types. It was observed that the velocity is effaced with the nanofluid type. Abu-Nada (2008) performed numerical study of convection over a backward-facing step using different nanofluid types. It was reported that nanoparticles having lower thermal conductivity perform better heat transfer performance in the recirculation region, but the average heat transfer enhances with the nanoparticle volume fraction. When magnetic field was used with electrical conductive fluids, nanoparticles change the electrical conductivity of the base fluid. When nanoparticles are included to the base fluid, both thermal conductivity and electrical conductivity are

enhanced, and therefore, their combined effect (magnetic field effects + nanoparticle addition) on the convective heat transfer characteristics may be favorable or detrimental depending on the application.

In this study, forced convection of nanofluid flow in a branching channel under the effect of magnetic field was numerically studied. Magnetic field effects with nanoparticle inclusion to the base fluid on the convective heat transfer was analyzed for various inclination angles of the lower branching channel. Flow separation at the junction of the channels and thus convective heat transfer rate are influenced by the variation of these parameters. There are many studies related to application of the magnetic field with nanofluids, and a few of them are related to configurations with separated flows. To the best of our knowledge, there exist no studies for the application of nanofluids and magnetic field for the convective heat transfer in a branching channel. This topic is of importance as there are many engineering application of the branching channels as mentioned above. The use of magnetic field and enhancement in both the thermal conductivity and electrical conductivity with the inclusion of the nanoparticles provide favorable thermophysical properties of the nanofluid when it used as a heat transfer fluid in a branching channel. The results of this study may be used to control the thermal performance in a branching channel and further optimization studies in the presence of magnetic field.

2. Modeling

Figure 1(a) presents the schematic view of physical model with boundary conditions. A branching channel is considered and the lower branching channel makes an angle of θ with the horizontal axis. The length and height of the channels are L and D with the sub-indices 1, 2 and 3 designating for the main, upper and lower channels. Nanofluid with velocity u_0 and temperature T_c is emerged from inlet of the main channel. The length and height ratio of the channels are 60 for each of the three channels. The walls of the channels are kept at constant temperature of T_h. A uniform magnetic field with strength of B_0 is imposed. Various effects such as joule heating, displacement currents, induced magnetic field, thermal radiation and viscous dissipation were assumed to be neglected. As the heat transfer fluid, water with various solid particle volume fraction of CuO nanoparticles was utilized. The nanoparticle is spherical shaped and has an average diameter of 30 nm. Table I presents various thermophysical properties of water CuO nanoparticle at reference temperature.

Mass, momentum and energy conservation equations in a 2D Cartesian coordinate system for laminar, steady flow and with the above-mentioned assumptions can be written as:

$$\frac{\partial u}{\partial x}+\frac{\partial v}{\partial y}=0 \tag{1}$$

$$u\frac{\partial u}{\partial x}+v\frac{\partial u}{\partial y}=-\frac{1}{\rho_{\mathrm{nf}}}\frac{\partial p}{\partial x}+\nu_{\mathrm{nf}}\left(\frac{\partial^2 u}{\partial x^2}+\frac{\partial^2 u}{\partial y^2}\right)+\frac{\sigma_{nf}B_0^2}{\rho_{nf}}\left(v\sin(\gamma)\cos(\gamma)-u\sin^2(\gamma)\right) \tag{2}$$

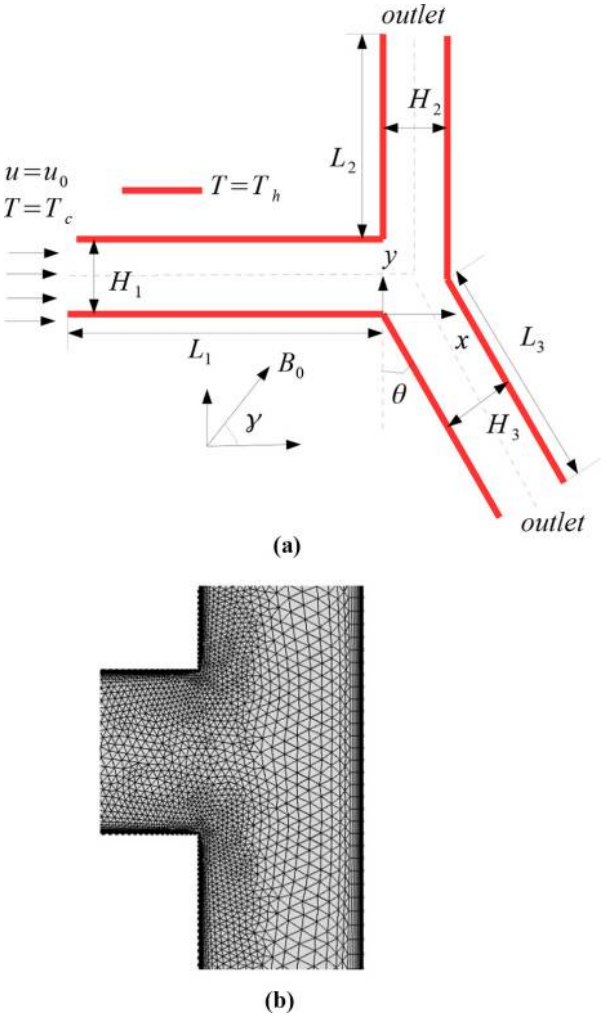

Figure 1.
Schematic description of the physical model (a) and grid distribution (b)

Property	Water	CuO
ρ (kg/m^3)	997.1	6,500
c_p (J/kg K)	4179	540
k (W/mK)	0.61	18
σ (S/m)	0.05	5×10^7
d_p (mm)	–	29

Source: Mahmoudi *et al.*, 2012

Table I.
Thermophysical properties of base fluid and nanoparticle

$$u\frac{\partial v}{\partial x}+v\frac{\partial v}{\partial y}=-\frac{1}{\rho_{\mathrm{nf}}}\frac{\partial p}{\partial y}+\nu_{\mathrm{nf}}\left(\frac{\partial^2 v}{\partial x^2}+\frac{\partial^2 v}{\partial y^2}\right)$$
$$+\frac{\sigma_{nf}B_0^2}{\rho_{nf}}\left(u\sin(\gamma)\cos(\gamma)-v\cos^2(\gamma)\right) \tag{3}$$

$$u\frac{\partial T}{\partial x}+v\frac{\partial T}{\partial y}=\alpha_{\mathrm{nf}}\left(\frac{\partial^2 T}{\partial x^2}+\frac{\partial^2 T}{\partial y^2}\right) \tag{4}$$

Equations (1)-(4) can be converted in dimensionless form by using the following dimensionless parameters:

$$X=\frac{x}{H},\ Y=\frac{y}{H},\ U=\frac{u}{u_0},\ V=\frac{v}{u_0},$$
$$P=\frac{p}{\rho_f u_0^2},\ \theta=\frac{T-T_c}{T_h-T_c},\ \mathrm{Pr}=\frac{\nu_f}{\alpha_f}, \tag{5}$$
$$\mathrm{Ha}=B_0H\sqrt{\frac{\sigma_f}{\mu_f}},\ \mathrm{Re}=\frac{u_0H}{\nu_f}$$

Dimensional form of the boundary conditions are expressed as following:

- At the inlet of the main channel, velocity is unidirectional and temperature is uniform, $u = u_0$, $v = 0$, $T = T_c$.
- On the walls of all channels, temperature is constant, $T = T_h$.
- At the exit of the branching channels, outflow boundary conditions are used, $\frac{\partial u_1}{\partial n}=0,\ u_2=0,\ \frac{\partial \theta}{\partial n}=0$.

2.1 Correlations for the calculation of nanofluid thermophysical effective properties

Nanofluid effective density and specific heat are defined as:

$$\rho_{nf}=(1-\phi)\rho_f+\phi\rho_{np}, \tag{6}$$

$$(\rho C_p)_{nf}=(1-\phi)(\rho C_p)_f+\phi(\rho C_p)_{np}. \tag{7}$$

Nanofluid thermal conductivity is described as follows:

$$k_{nf}=k_f\left[\frac{(k_p+2k_f)-2\phi(k_f-k_p)}{(k_p+2k_f)+\phi(k_f-k_p)}\right]+5\times10^4\phi\rho_f c_{p,f}\sqrt{\frac{\kappa_b T}{\rho_p d_p}}\,g(T,\phi,d_p) \tag{8}$$

where the first term on the tight hand side is the static thermal conductivity as given by Maxwell (1873) and the effects of temperature are included in the models via the second term of the above equation. The form of the function g is given in Koo and Kleinstreuer, 2005.

This model takes into account the Brownian motion. In this model, particle size (d_p), particle volume fraction (ϕ) and temperature (T) effects are considered.

The effective viscosity of the nanofluid is given by (Koo and Kleinstreuer, 2005):

$$\mu_{nf} = \frac{\mu_f}{(1-\phi)^{0.25}} + \frac{k_{Brownian}}{k_f} \times \frac{\mu_f}{Pr_f} \tag{9}$$

where the first term on the right hand side of equation is the viscosity of the nanofluid defined in (Brinkman, 1952).

Maxwell's model (Maxwell, 1873) was used for the electrical conductivity of the nanofluid, which is given as:

$$\sigma_{nf} = \sigma_f \left(1 + \frac{3(f-1)\phi}{(f+2) - (f-1)\phi}\right) \tag{10}$$

where $f = \frac{\sigma_p}{\sigma_f}$ is the conductivity ratio of the two phases. It is developed for electrical conductivity of random suspension of spherical particles (Maxwell, 1873). Effects of different electrical conductivity models of Al_2O_3-water nanofluid in a mixed convection study was discussed in (Selimefendigil and Oztop, 2018).

2.2 Solver and the validation of the present code

Galerkin weighted residual finite element method was used for the solution of the equations with boundary conditions. In this method, residual R is obtained when the approximated flow field variables are inserted into the governing equations. The weighted average of the residual is forced to be zero over the computational domain:

$$\int_{\Omega} w_k R dv = 0 \tag{11}$$

where w_k is the weight function. The weight function is chosen from the same set of functions as of the trial functions. The resulting system of nonlinear ordinary differential equations is solved with Newton–Raphson method.

Numerical tests with various number of triangular elements were performed to obtain grid independence solution. Table II shows the results of average Nusselt number along the hot walls for various grid sizes at two different solid nanoparticle volume fraction (Re = 500, Ha = 15, $\theta = 0^{\circ}$). G5 with 74,809 number of triangular elements was chosen. A grid distribution of the computational domain is shown in Figure 1(b). Validation of the code is made against the analytical results of Luo *et al.* (2018), in which a theoretical study for the

Grid name	No. of elements	Nu_m ($\phi = 0$)	Nu_m ($\phi = 0.04$)
G1	2,772	5.549	7.043
G2	4,614	4.754	5.976
G3	9,062	3.619	4.423
G4	39,227	3.512	4.259
G5	74,809	3.412	4.142
G6	112,117	3.403	4.139

Table II. Grid independence study (Re = 500, Ha = 15)

heat transfer in a branch network was performed. Table III shows the heat transfer rate calculated by using several pipe diameters and calculated with the present solver and obtained with the model in Luo *et al.* (2018). Another validation of the present code is made with existing results of Khandelwal *et al.* (2015), in which non-Newtonian fluid flow in a right-angled T-channel was numerically studied. Recirculation lengths calculated at two different Reynolds number are shown in Table IV.

3. Results and discussion

In the present study, convective heat transfer characteristics of CuO-water nanofluid in a branching channel was investigated under the effect of magnetic field. A uniform horizontally aligned magnetic field ($\gamma = 0°$) was imposed, and the angle of lower branching channel that it makes with the vertical axis is θ. The heat transfer and fluid flow characteristics are influenced by geometry of the configuration, flow conditions and thermophysical properties of the fluid. In the current investigation, the geometrical change of the configuration is attained by changing the angle θ of the lower branching channel and thermophysical properties are affected by introducing solid nanoparticles to the base fluid. Numerical simulations for various values of Reynolds number (between 100 and 500), Hartmann number (between 0 and 15), nanoparticle solid volume fraction (between 0 and 0.04) and branching angle of the lower channel (between 0 and 90) were performed. Results are illustrated with streamline, isotherm, local and average Nusselt number distributions for various values of investigated parameters.

3.1 Flow and thermal patterns

3.1.1 Effects of Reynolds number. Flow and thermal patterns for various values of Reynolds number and for three different inclination angle of lower branching channel are demonstrated in Figures 2 and 3. The flow is separated at the edges of the walls for the upper and lower branching channel when $\theta = 0°$ and $\theta = 45°$. As the Reynolds number is increased, recirculation regions enhances and this is more effective for the upper channel at $\theta = 0°$. The increase of the recirculation length with Reynolds number has been previously

Table III.
Code validation 1: comparison of heat transfer rate for different trunk diameters computed in (Luo *et al.*, 2018) and obtained with the present solver

d (m)	Reference	Present solver	Difference (%)
0.0010	0.32	0.34	6.25
0.0034	41.25	43.35	5.09
0.0040	67.5	64.05	−5.11

Table IV.
Code validation 2: comparison of the recirculation lengths in a right-angled T-channel

Re	L_R/D (Khandelwal *et al.*, 2015)	L_R/D (present)	Difference (%)
25	1.44	1.38	−4.17
200	3.99	3.96	−0.75

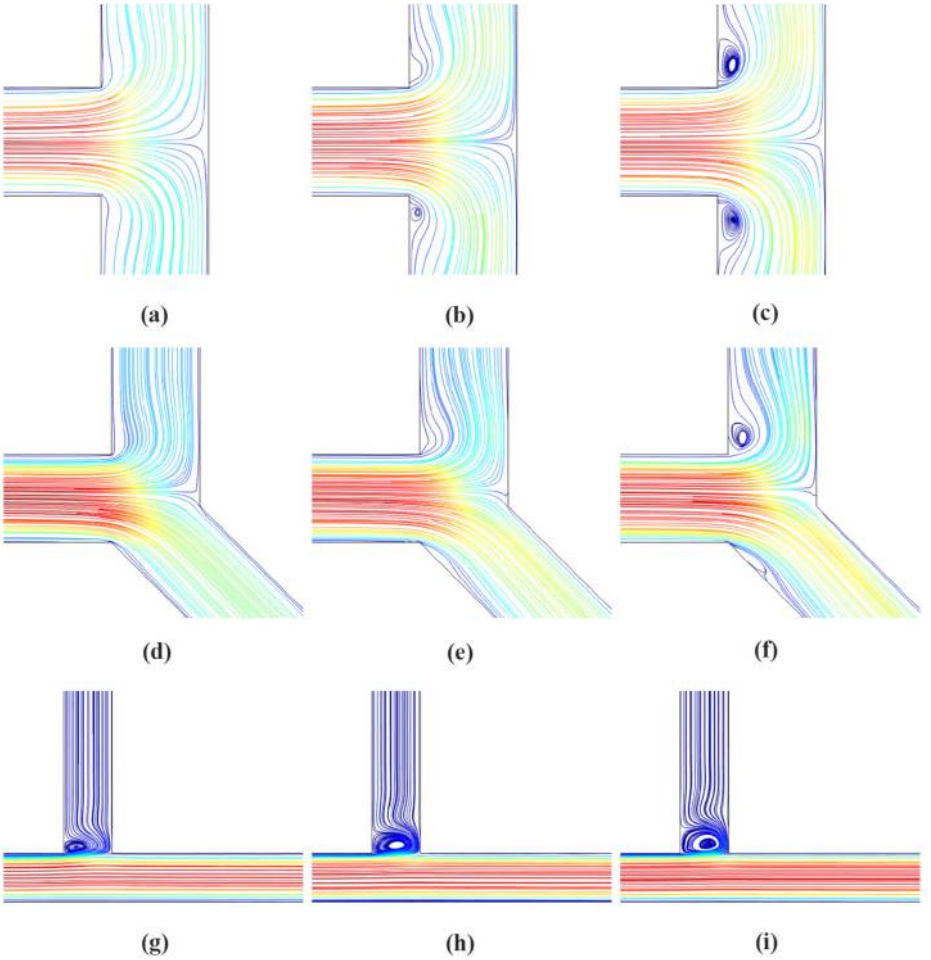

Notes: (a) Re = 100, $\theta = 0^{\circ}$ (b) Re = 300, $\theta = 0^{\circ}$ (c) Re = 500, $\theta = 0^{\circ}$; (d) Re = 100, $\theta = 45^{\circ}$; (e) Re = 300, $\theta = 45^{\circ}$; (f) Re = 500, $\theta = 45^{\circ}$; (g) Re = 100, $\theta = 90^{\circ}$; (h) Re = 300, $\theta = 90^{\circ}$; (i) Re = 500, $\theta = 90^{\circ}$

Figure 2.
Variation of streamlines for different values of Reynolds number and various values of branching angle (Ha = 5, ϕ = 0.02)

obtained in various studies for the separated flow over a backward-facing step. When the lower branching channel is horizontally aligned for θ = 90°, a weak recirculation zone is established in the upper channel, but this occupies a large portion of the upper channel height. Table V shows the reattachment length for the upper branching channel for two different branching angles (Ha = 5, ϕ = 0.04). For the horizontal alignment of the lower channel (θ = 90°), reattachment length is higher as compared to vertical alignment (θ = 90°). Reattachment lengths increase with the augmentation of the Reynolds number, and 31.81 and 19.30 per cent enhancements are obtained when Reynolds number is increased from 100 to 500 at θ = 0° and 90°, respectively. Isotherms become denser along the walls of

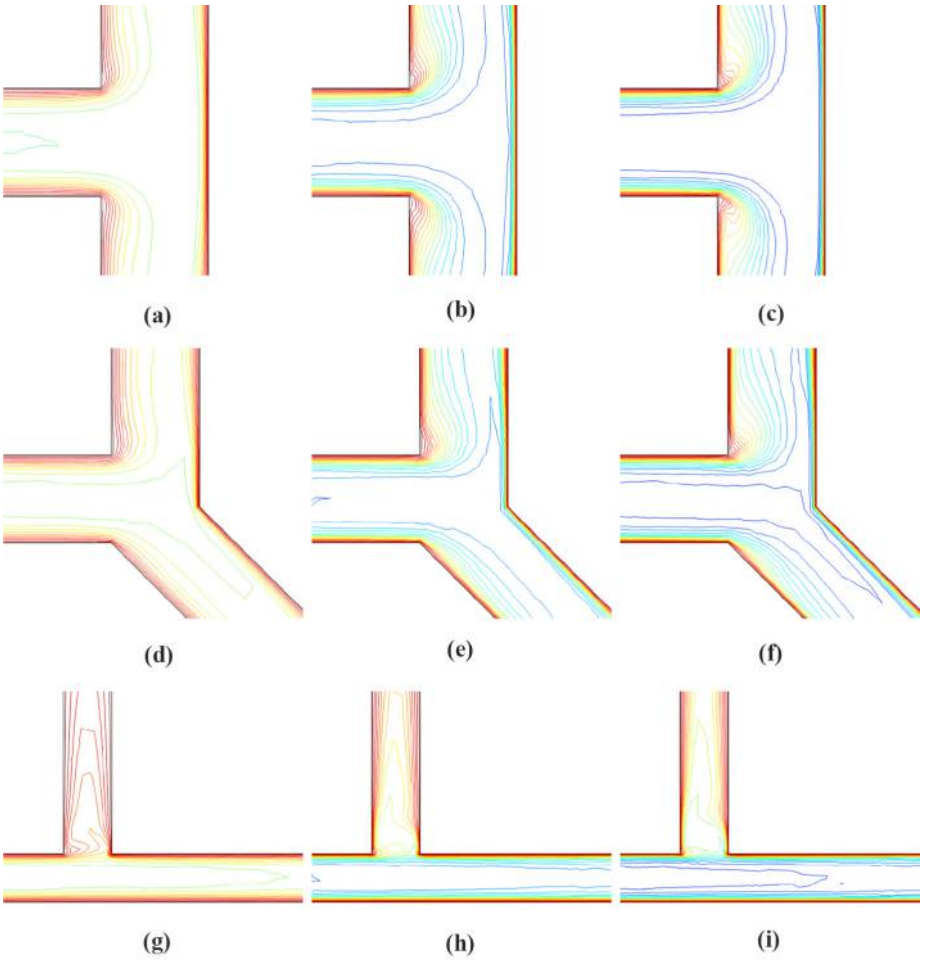

Figure 3.
Distribution of isotherms for different values of Reynolds number and various values of branching angle (Ha = 5, ϕ = 0.02)

Notes: (a) Re = 100, $\theta = 0^{\circ}$ (b) Re = 300, $\theta = 0^{\circ}$ (c) Re = 500, $\theta = 0^{\circ}$; (d) Re = 100, $\theta = 45^{\circ}$; (e) Re = 300, $\theta = 45^{\circ}$; (f) Re = 500, $\theta = 45^{\circ}$; (g) Re = 100, $\theta = 90^{\circ}$; (h) Re = 300, $\theta = 90^{\circ}$; (i) Re = 500, $\theta = 90^{\circ}$

Table V.
Effects of Reynolds number on the reattachment length of the upper branching channel for two different branching angles (Ha = 5, ϕ = 0.02)

Re	$\theta = 0°$	$\theta = 90°$
100	1.10	1.29
200	1.19	1.36
300	1.25	1.41
400	1.38	1.50
500	1.45	1.54

the channel with higher values of Reynolds number indicating the enhanced heat transfer. Steep temperature gradients are observed near the reattachment points for the separated flow at the edges of the upper and lower branching channels.

3.1.2 Effects of Hartmann number. Streamline distributions for different inclination angles of the lower branching channel are shown in Figure 4 under the effect of magnetic field. Magnetic field strength is characterized by Hartmann number and Ha = 0 denotes the absence of the magnetic field. Magnetic field was shown to suppress the fluid motion and reduces the convective heat transfer in many configurations. As it is shown in several studies, magnetic field could also act in a way to reduce the recirculation length and enhance the heat transfer as those encountered in separated flows. In the absence of magnetic field

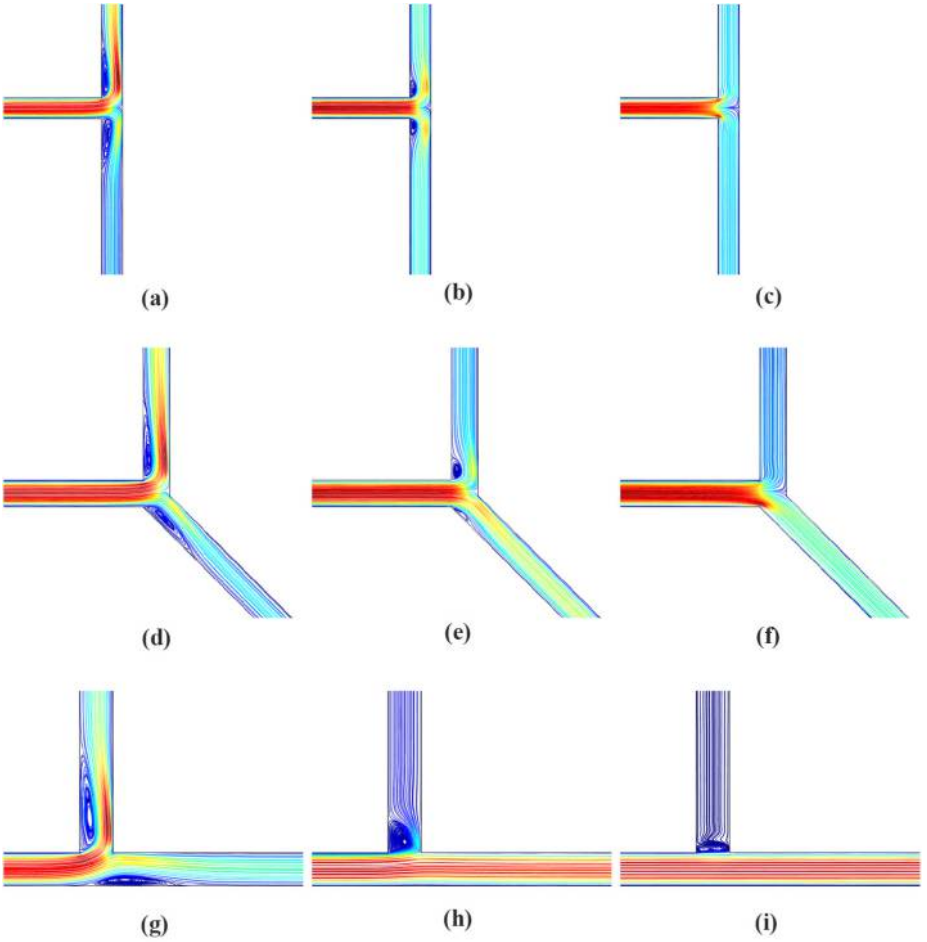

Notes: (a) Ha = 0, $\theta = 0°$; (b) Ha = 2.5, $\theta = 0°$; (c) Ha = 15, $\theta = 0°$; (d) Ha = 0, $\theta = 45°$; (e) Ha = 2.5, $\theta = 45°$; (f) Ha = 15, $\theta = 45°$; (g) Ha = 0, $\theta = 90°$; (h) Ha = 2.5, $\theta = 90°$; (i) Ha = 15, $\theta = 90°$

Figure 4.
Effects of Hartmann number on the variation of streamlines for different branching angles ($\phi = 0.02$)

(Ha = 0), recirculation zones are established in the upper wall of the upper branching channel and in the lower wall of the lower branching channel. As the magnetic field strength is increased via Hartmann number, recirculation zones in the branching channels gradually decrease and at Ha = 15, they disappear for $\theta = 0°$ and $\theta = 45°$. For the horizontal alignment of the lower branching channel, fluid flow is significantly reduced in the upper channel, but the recirculation zone in the upper channel is also reduced with the magnetic field. Table VI shows the influence of Hartmann number on the reattachment length of the upper branching channel for two different θ values. Reattachment length deceases for higher magnetic field strength due to the suppression of vortex in the upper branching channel. The value of reattachment length is higher for horizontal alignment of the lower branching channel.

3.2 Nusselt number variations

Variation of the average Nusselt number for various channels (denoted by P1, P2 and P3) are shown in Figure 5(a) and (b). Average heat transfer enhances with the increment in the Reynolds number and adding nanoparticle addition results in higher heat transfer rates due to the higher thermal conductivity of the nanofluid. The trends in the average Nusselt number is similar for nanofluid considering different nanoparticle volume fractions. At Reynolds number of 100 and 400, average Nusselt number enhancements of 24.50 and 20.43 per cent, respectively, are achieved for nanofluid with highest solid particle as compared to pure water.

Effects of inclination angle of the lower branching channel on the distribution of the average Nusselt number are demonstrated in Figure 6 for various nanoparticle solid volume fractions. Average Nusselt number increases with higher θ values up to $\theta = 60°$ and decreases thereafter. Table VII shows the effects of inclination angle of the branching channel on the variation of the average Nusselt number for each of the channels (Re = 300, Ha = 5, $\phi = 0.04$). For the configurations shown in the Table VII, heat transfer is significantly reduced for the upper channel at $\theta = 90°$ due to the occurrence of the vortex which occupies the large portion of the channel and restricts the fluid motion through upper branching channel. Average Nusselt number is linearly varying with solid nanoparticle volume fraction for all inclination angles. Average Nusselt number increases by 24.16 and 20.00 per cent for inclination angles of $\theta = 60°$ and $\theta = 90°$, at the highest value of solid particle volume fraction.

Variation of the average Nusselt number versus Hartmann number is demonstrated in Figure 7 (Re = 300, $\theta = 45°$) when nanofluid with all solid particle volume fractions is considered. Average Nusselt number is an increasing function of Hartmann number and solid particle volume fraction. A higher value of Hartmann number results in suppression of the recirculation zone behind the separated edge and the inclusion of the

Table VI.
Effects of Hartmann number on the reattachment length of the upper branching channel for two different branching angles (Re = 300, $\phi = 0.02$)

Ha	$\theta = 0°$	$\theta = 90°$
0	3.50	4.10
2.5	1.88	1.95
5	1.25	1.40
10	1.15	1.29
15	1.10	1.28

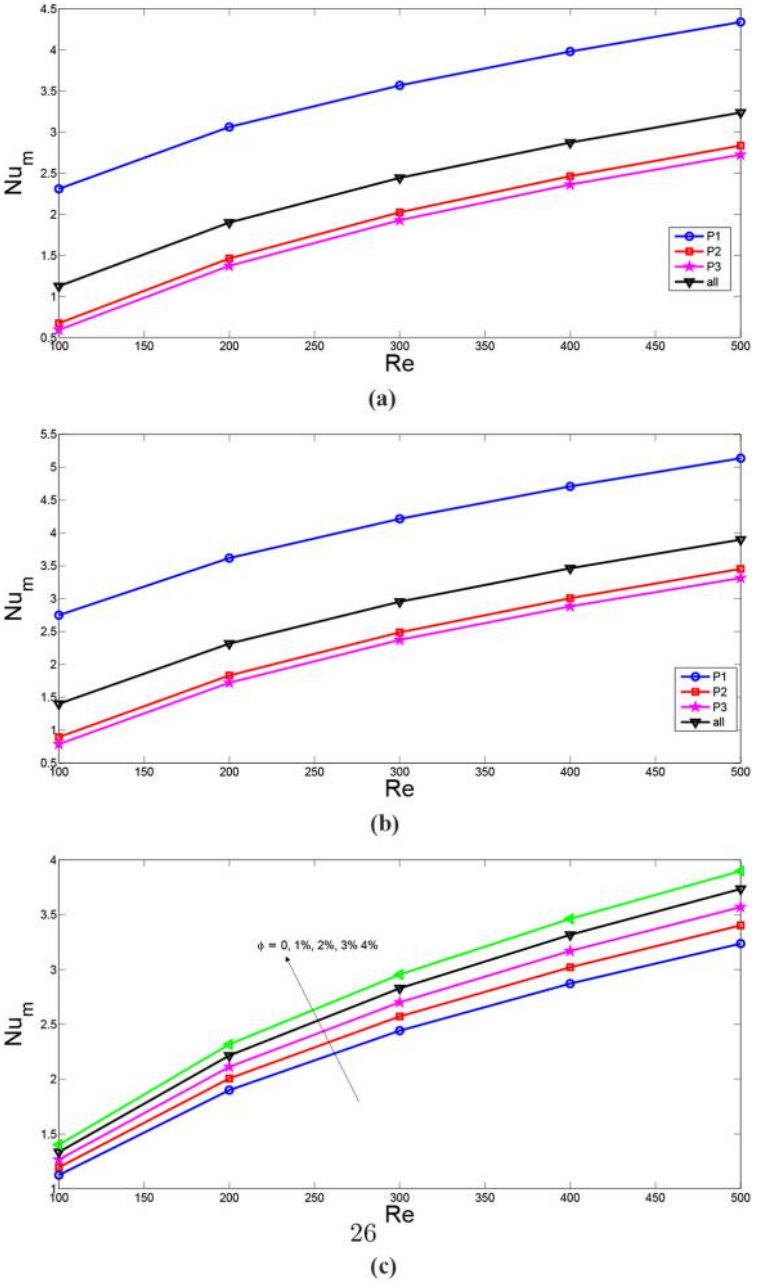

Figure 5.
Average Nusselt number versus Reynolds number for different branches of the channel at $\phi = 0$ (a), $\phi = 0.04$ (a) and for all nanoparticle solid volume fraction (c) (Ha = 5)

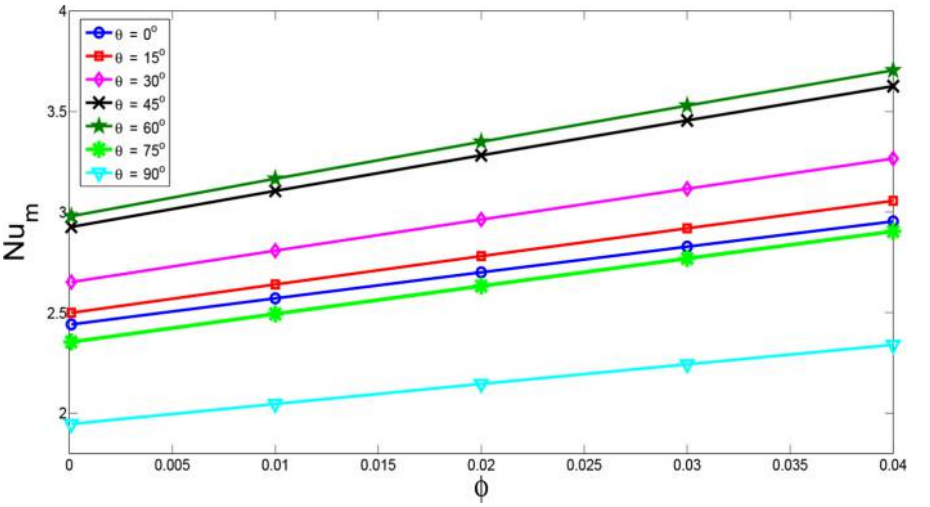

Figure 6.
Average Nusselt number versus solid nanoparticle volume fraction for different inclination angles of the lower branching channel (Re = 300, Ha = 5)

Table VII.
Effects of inclination angle of the branching channel for variation of the average nusselt number in different channels (Re = 300, Ha = 5, ϕ = 0.04)

θ (deg)	P1	P2	P3	Overall
0	4.215	2.487	2.373	2.953
60	4.296	1.485	5.449	3.705
90	4.393	0.288	2.684	2.340

nanofluid results in both thermal conductivity and electrical conductivity enhancements of the base fluid. Therefore, it is expected that a higher value of magnetic field strength and solid particle volume fraction results in highest value of heat transfer. Table VIII shows the average heat transfer enhancement of nanofluid with the highest particle volume fraction as compared to pure water in the absence and presence of magnetic field for different inclination angle of the lower branching channel. Including nanoparticle to the base fluid is effective for the case when heat transfer is higher (higher value of Hartmann number) and the discrepancy between the average heat transfer is higher (with and without magnetic field) when the inclination angle of the lower branching channel is $\theta = 45°$.

4. Conclusions

Numerical simulation of forced convection of nanofluid flow in a branching channel was performed under the influence of magnetic field. The inclination angle of the lower branching channel, thermophysical properties of the fluid via inclusion of nanoparticles and magnetic field strength were changed, and effects of these parameters on the fluid flow and

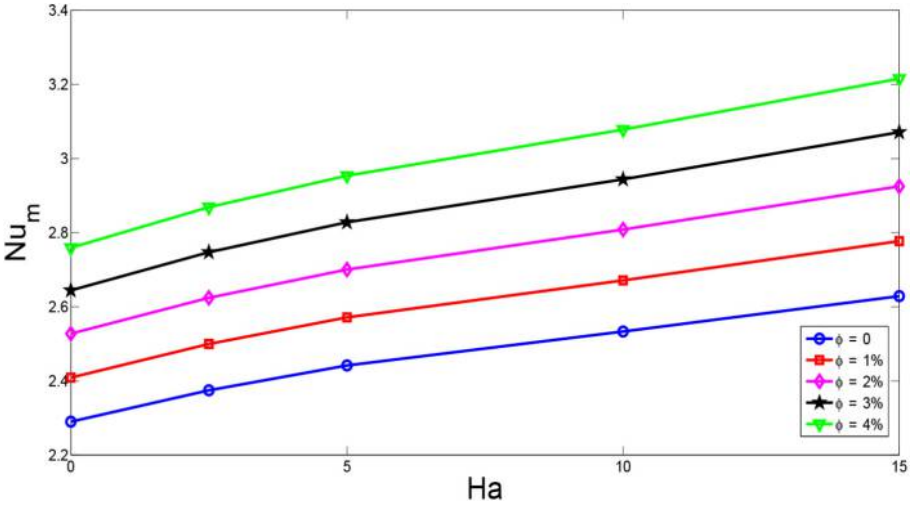

Figure 7.
Variation of average Nusselt number versus Hartmann number for all nanoparticle solid volume fractions (Re = 300)

Table VIII.
Average Nusselt number enhancement for nanofluid at highest volume fraction as compared to water in the absence and presence of magnetic field (Re = 300)

Ha	$\theta = 0°$ (%)	$\theta = 45°$ (%)	$\theta = 90°$ (%)
0	21.22	15.26	15.20
15	22.33	22.35	20.1

heat transfer characteristics were analyzed. Several important remarks can be concluded as follows:

- Reattachment lengths enhance with the augmentation of the Reynolds number. The average Nusselt number increases for higher values of Reynolds number and adding nanoparticles.
- The average heat transfer enhances with higher inclination angle of the lower branching channel for values up to 60° and reduces thereafter, which is due to the occurrence of the large vortex in the upper branching channel.
- The reattachment length reduces for higher values of Hartmann number, which is due to the suppression of vortex in the upper branching channel.
- Higher values of Hartmann number and solid particle volume fraction result in higher values of average Nusselt number.
- The discrepancy between the average Nusselt number is higher when the inclination angle of the lower branching channel is 45° both in the absence and presence of the magnetic field.

References

Al-aswadi, A.A., H.A., Mohammed, N.H. Shuaib. and AntonioCampo, (2010), "Laminar forced convection flow over a backward facing step using nanofluids", *International Communications in Heat and Mass Transfer*, Vol. 37 No. 8, pp. 950-957.

Abu-Mulaweh, H. (2003), "A review of research on laminar mixed convection flow over backward- and forward facing steps", *International Journal of Thermal Sciences*, Vol. 42 No. 9, pp. 897-909.

Abu-Nada, E. (2008), "Application of nanofluids for heat transfer enhancement of separated flows encountered in a backward facing step", *International Journal of Heat and Fluid Flow*, Vol. 29 No. 1, pp. 242-249.

Abu-Nada, E. and Chamkha, A.J. (2010), "Mixed convection flow in a lid-driven inclined square enclosure filled with a nanofluid", *European Journal of Mechanics B/Fluids*, Vol. 29 No. 6, pp. 472-482.

Armaghani, T., Chamkha, A.J., Maghrebi, M. and Nazari, M. (2014), "Numerical analysis of a nanofluid forced convection in a porous channel: a new heat flux model in ltne condition", *Journal of Porous Media*, Vol. 17 No. 7, pp. 637-646.

Brinkman, H. (1952), "The viscosity of concentrated suspensions and solutions", *Journal of Chemical Physics*, Vol. 20 No. 4, pp. 571-581.

Chiang, T.P. and Sheu, T.W.H. (1999), "A numerical revisit of backward-facing step flow problem", *Phys. Fluids*, Vol. 11 No. 4, pp. 862-874.

Dyne, B., Pepper, D. and Brueckner, F. (1993), "Mixed convection in a vertical channel with a backward-facing step", *ASME HTD*, Vol. 258.

Esmaeilpour, M. and Abdollahzadeh, M. (2012), "Free convection and entropy generation of nanofluid inside an enclosure with different patterns of vertical wavy walls", *International Journal of Thermal Sciences*, Vol. 52, pp. 127-136.

Hossain, M.S. and Alim, M.A. (2014), "Mhd free convection within trapezoidal cavity with non-uniformly heated bottom wall", *International Journal of Heat and Mass Transfer*, Vol. 69, pp. 327-336.

Ishak, A., Nazar, R. and Pop, I. (2009), "Mhd convective flow adjacent to a vertical surface with prescribed wall heat flux", *International Communications in Heat and Mass Transfer*, Vol. 36 No. 6, pp. 554-557.

Jang, J. and Hsu, C.T. (2009), "Vortex instability of mhd natural convection flow over a horizontal plate in a porous medium", *Computers and Fluids*, Vol. 38 No. 2, pp. 333-339.

Kaiktsis, L., Karniadakis, G.E. and Orszag, S.A. (1991), "Onset of three-dimensionality, equilibria, and early transition in flow over a backward-facing step", *Journal of Fluid Mechanics*, Vol. 231 No. 1, pp. 501-528.

Khandelwal, V., Dhiman, A. and Baranyi, L. (2015), "Laminar flow of non-newtonian shear-thinning fluids in a t-channel", *Computers and Fluids*, Vol. 108, pp. 79-91.

Khodadadi, J.M., Nguyen, T.M. and Vlachos, N.S. (1986), "Laminar forced convective heat transfer in a two-dimensional 90 deg bifurcation", *Numerical Heat Transfer*, Vol. 9 No. 6, pp. 677-695.

Khodadadi, J.M., Vlachos, N.S., Liepsch, D. and Moravec, S. (1988), "Lda measurements and numerical prediction of pulsatile laminar flow in a plane 90-degree bifurcation", *Journal of Biomechanical Engineering*, Vol. 110 No. 2, pp. 129-136.

Koo, J. and Kleinstreuer, C. (2005), "Laminar nanofluid flow in microheat-sinks", *International Journal of Heat and Mass Transfer*, Vol. 48 No. 13, pp. 2652-2661.

Lee, H.G., Ha, M.Y. and Yoon, H.S. (2005), "A numerical study on the fluid flow and heat transfer in the confined jet flow in the presence of magnetic field", *International Journal of Heat and Mass Transfer*, Vol. 48 Nos 25/26, pp. 5297-5309.

Lin, J., Armaly, B. and Chen, T. (1990), "Mixed convection in buoyancy-assisted vertical backward-facing step flows", *International Journal of Heat and Mass Transfer*, Vol. 33 No. 10, pp. 2121-2132.

Luo, L., Tian, F., Cai, J. and Hu, X. (2018), "The convective heat transfer of branched structure", *International Journal of Heat and Mass Transfer*, Vol. 116, pp. 813-816.

Maghrebi, M.J., Nazari, M. and Armaghani, T. (2012), *Forced Convection Heat Transfer of Nanofluids in a Porous Channel*, Transport in Porous Media.

Mahmoudi, A.H., Pop, I. and Shahi, M. (2012), "Effect of magnetic field on natural convection in a triangular enclosure filled with nanofluid", *International Journal of Thermal Sciences*, Vol. 59, pp. 12-140.

Matos, H. and Oliveira, P. (2013), "Steady and unsteady non-newtonian inelastic flows in a planar t-junction", *International Journal of Heat and Fluid Flow*, Vol. 39, pp. 102-126.

Maxwell, J. (1873), *A Treatise on Electricity and Magnetism*, Oxford University Press.

Nie, J. and Armaly, B. (2004), "Convection in laminar three-dimensional separated flow", *International Journal of Heat and Mass Transfer*, Vol. 47 No. 25, pp. 5407-5416.

Oztop, H.F. and Abu-Nada, E. (2008), "Numerical study of natural convection in partially heated rectangular enclosures filled with nanofluids", *International Journal of Heat and Fluid Flow*, Vol. 29 No. 5, pp. 1326-1336.

Oztop, H.F., Rahman, M., Ahsan, A., Hasanuzzaman, M., Saidur, R., Al-Salem, K., Rahim, N., (2012), "Mhd natural convection in an enclosure from two semi-circular heaters on the bottom wall", *International Journal of Heat and Mass Transfer*, Vol. 55 pp. 1844-1854.

Rahman, M., Oztop, H.F., Saidur, R., Mekhilef, S. and Al-Salem, K. (2013), "Finite element solution of mhd mixed convection in a channel with a fully or partially heated cavity", *Computers and Fluids*, Vol. 79, pp. 53-64.

Sarris, I., Zikos, G., Grecos, A. and Vlachos, N. (2006), "On the limits of validity of the low magnetic reynolds number approximation in mhd natural-convection heat transfer", *Numer. Heat Transfer Part B*, Vol. 50, pp. 158-180.

Saryazdi, A.B., Talebi, F., Armaghani, T. and Pop, I. (2016), "Numerical study of forced convection flow and heat transfer of a nanofluid flowing inside a straight circular pipe filled with a saturated porous medium", *The European Physical Journal Plus*, Vol. 131, pp. 78-88.

Selimefendigil, F. and Chamkha, A.J. (2016), "Magnetohydrodynamics mixed convection in a lid-driven cavity having a corrugated bottom wall and filled with a non-newtonian power-law fluid under the influence of an inclined magnetic field", *Journal of Thermal Science and Engineering Applications*, Vol. 8 No. 2, p. 021023.

Selimefendigil, F. and Oztop, H.F. (2014a), "Control of laminar pulsating flow and heat transfer in backward-facing step by using a square obstacle", *Journal of Heat Transfer*, Vol. 136 No. 8, p. 081701.

Selimefendigil, F. and Oztop, H.F. (2013a), "Identification of forced convection in pulsating flow at a backward facing step with a stationary cylinder subjected to nanofluid", *International Communications in Heat and Mass Transfer*, Vol. 45, pp. 111-121.

Selimefendigil, F. and Oztop, H.F. (2014b), "Pulsating nanofluids jet impingement cooling of a heated horizontal surface", *International Journal of Heat and Mass Transfer*, Vol. 69, pp. 54-65.

Selimefendigil, F. and Oztop, H.F. (2015a), "Influence of inclination angle of magnetic field on mixed convection of nanofluid flow over a backward facing step and entropy generation", *Advanced Powder Technology*, Vol. 26 No. 6, pp. 1663-1675.

Selimefendigil, F. and Oztop, H.F. (2015b), "Mixed convection in a two-sided elastic walled and sio2 nanofluid filled cavity with internal heat generation: Effects of inner rotating cylinder and nanoparticle's shape", *Journal of Molecular Liquids*, Vol. 212, pp. 509-516.

Selimefendigil, F. and Oztop, H.F. (2017), "Effects of nanoparticle shape on slot-jet impingement cooling of a corrugated surface with nanofluids", *Journal of Thermal Science and Engineering Applications*, Vol. 9 No. 2, pp. 021016-021018.

Selimefendigil, F. and Oztop, H.F. (2018), "Modeling and optimization of mhd mixed convection in a lid-driven trapezoidal cavity filled with alumina-water nanofluid: effects of electrical conductivity models", *International Journal of Mechanical Sciences*, Vol. 136, pp. 264-278.

Selimefendigil, F., Ismael, M.A. and Chamkha, A.J. (2017), "Mixed convection in superposed nanofluid and porous layers in square enclosure with inner rotating cylinder", *International Journal of Mechanical Sciences*, Vol. 124, pp. 95-108.

Senn, S. and Poulikakos, D. (2004), "Laminar mixing, heat transfer and pressure drop in tree-like microchannel nets and their application for thermal management in polymer electrolyte fuel cells", *Journal of Power Sources*, Vol. 130 Nos 1/2, pp. 178-191.

Sivasankaran, S., Mansour, M.A., Rashad, A.M. and Bhuvaneswari, M. (2016), "Mhd mixed convection of cu-water nanofluid in a two-sided lid-driven porous cavity with a partial slip", *Numerical Heat Transfer, Part A*, Vol. 70 No. 12, pp. 1356-1370.

Terhaar, S., Velazquez, A., Arias, J. and Sanchez-Sanz, M. (2010), "Experimental study on the unsteady laminar heat transfer downstream of a backwards facing step", *International Communications in Heat and Mass Transfer*, Vol. 37 No. 5, pp. 457-462.

Wang, X.Q., Xu, P., Mujumdar, A.S. and Yap, C. (2010), "Flow and thermal characteristics of offset branching network", *International Journal of Thermal Sciences*, Vol. 49 No. 2, pp. 272-280.

Williams, P.T. and Baker, A.J. (1997), "Numerical simulations of laminar flow over a 3d backward-facing step", *International Journal for Numerical Methods in Fluids*, Vol. 24 No. 11, pp. 1159-1183.

Further reading

Rashad, A.M., Ismael, M.A., Chamkha, A.J. and Mansour, M.A. (2016), "Mhd mixed convection of localized heat source/sink in a nanofluid-filled lid-driven square cavity with partial slip", *Journal of the Taiwan Institute of Chemical Engineers*, Vol. 68, pp. 173-186.

Rashad, A.M., Sivasankaran, S., Mansour, M.A. and Bhuvaneswari, M. (2017), "Magneto-convection of nanofluids in a lid-driven trapezoidal cavity with internal heat generation and discrete heating", *Numerical Heat Transfer, Part A: Applications*, Vol. 71 No. 12, pp. 1223-1234.

Selimefendigil, F. and Oztop, H.F. (2013b), "Numerical analysis of laminar pulsating flow at a backward facing step with an upper wall mounted adiabatic thin fin", *Computers and fluids*, in press.

Corresponding author

Fatih Selimefendigil can be contacted at: fthsel@yahoo.com